

AD-762 347

SCALING OF GROUND MOTIONS FROM CONTAINED
EXPLOSIONS IN ROCK FOR ESTIMATING DIRECT
GROUND SHOCK FROM SURFACE BURSTS ON ROCK

Alfred J. Hendron, Jr.

Alfred J. Hendron

Prepared for.

Office of the Chief of Engineers

January 1973

DISTRIBUTED BY:

NTIS

National Technical Information Service
U. S. DEPARTMENT OF COMMERCE
5285 Port Royal Road, Springfield Va. 22151

AD

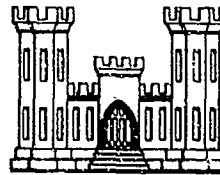
TECHNICAL REPORT NO. 15

SCALING OF GROUND MOTIONS FROM
CONTAINED EXPLOSIONS IN ROCK FOR
ESTIMATING DIRECT GROUND SHOCK
FROM SURFACE BURSTS ON ROCK

by

ALFRED J. HENDRON, JR.

JANUARY 1973



OMAHA DISTRICT, CORPS OF ENGINEERS
OMAHA, NEBRASKA 68102

THIS RESEARCH WAS FUNDED BY OFFICE,
CHIEF OF ENGINEERS, DEPARTMENT OF THE ARMY

PREPARED UNDER CONTRACT DACA 45-69-C-0100
BY ALFRED J. HENDRON, MAHOMET, ILLINOIS

Reproduced by
NATIONAL TECHNICAL
INFORMATION SERVICE
U S Department of Commerce
Springfield VA 22151

Approved for public release; distribution unlimited

DDC
RECEIVED
JUN 22 1973
C

37

UNCLASSIFIED

Security Classification

DOCUMENT CONTROL DATA - R & D

(Security classification of title, body of abstract and indexing annotation must be entered when the overall report is classified)

1. ORIGINATING ACTIVITY (Corporate author) Omaha District, Corps of Engineers Omaha, Nebraska 68102		2a. REPORT SECURITY CLASSIFICATION UNCLASSIFIED	
		2b. GROUP	
3. REPORT TITLE Scaling of Ground Motions from Contained Explosions in Rock for Estimating Direct Ground Shock from Surface Bursts on Rock.			
4. DESCRIPTIVE NOTES (Type of report and inclusive dates) Final			
5. AUTHOR(S) (First name, middle initial, last name) Alfred J. Hendron, Jr.			
6. REPORT DATE January 1973	7a. TOTAL NO. OF PAGES 32	7b. NO. OF REFS 6	
8a. CONTRACT OR GRANT NO. DACA 45-69-C-0100		9a. ORIGINATOR'S REPORT NUMBER(S) Technical Report No. 15	
b. PROJECT NO. 4DM 78012A OW 1 DA-4-DM-78012-AOW-1		9b. OTHER REPORT NO(S) (Any other numbers that may be assigned this report)	
c. Task: 03			
d. Work Unit: 015			
10. DISTRIBUTION STATEMENT Approved for public release; distribution unlimited			
11. SUPPLEMENTARY NOTES Reference: Technical Report No. 10, same originating agency (H0-743 v3c)		12. SPONSORING MILITARY ACTIVITY Department of the Army Office of the Chief of Engineers Washington, D. C. 20315	
13. ABSTRACT In this report, a large number of motion measurements from contained explosions in various rock types were reviewed and presented. These data were interpreted in terms of dimensional analysis and other constraints necessary for dynamic consistency to yield scaling relations for estimating peak motions in various rock media from contained bursts. Suggestions are also given for estimating ground motions from direct induced ground shock resulting from a surface burst on rock.			

DD FORM 1473

REPLACES DD FORM 1473, 1 JAN 64, WHICH IS OBSOLETE FOR ARMY USE.

UNCLASSIFIED

Security Classification

UNCLASSIFIED

Security Classification

14.

KEY WORDS

Contained Bursts
Dimensional Analysis
Dynamic Motions
Ground Motions
Ground Shock
Rock Media
Scaling Explosions
Surface Bursts

LINK A

LINK B

LINK C

ROLE

WT

ROLE

WT

ROLE

WT

UNCLASSIFIED

Security Classification

TECHNICAL REPORT NO. 15

SCALING OF GROUND MOTIONS FROM
CONTAINED EXPLOSIONS IN ROCK
FOR ESTIMATING DIRECT GROUND
SHOCK FROM SURFACE BURSTS ON
ROCK

by

ALFRED J. HENDRON, JR.

JANUARY 1973

OMAHA DISTRICT, CORPS OF ENGINEERS
OMAHA, NEBRASKA 68102

THIS RESEARCH WAS FUNDED BY OFFICE, CHIEF OF ENGINEERS
DEPARTMENT OF THE ARMY

PREPARED UNDER CONTRACT DACA 45-69-C-0100
BY ALFRED J. HENDRON, MAHOMET, ILLINOIS

Approved for public release; distribution unlimited

ABSTRACT

In this report, a large number of motion measurements from contained explosions in various rock types were reviewed and presented. These data were interpreted in terms of dimensional analysis and other constraints necessary for dynamic consistency to yield scaling relations for estimating peak motions in various rock media from contained bursts. Suggestions are also given for estimating ground motions from direct induced ground shock resulting from a surface burst on rock.

PREFACE

This investigation was authorized by the Chief of Engineers (DAEN-MCE-D) and was performed in FY 71 and 72 under contract No. DACA 45-69-C-0100 between the Omaha District, Corps of Engineers and Dr. A. J. Hendron, Mahomet, Illinois. The work is part of a continuing effort to develop methods which can be used to design underground openings in jointed rock to survive the effects of nuclear weapons.

This report was prepared under the supervision of Dr. A. J. Hendron, Principal Investigator. During the work period covered by this report, Colonel B. P. Pendergrass and Colonel Alfred L. Griebeling were District Engineers; R. G. Burnett was Chief, Engineering Division, C. J. Distefano was Technical Monitor for the Omaha District under the general supervision of Kendall C. Fox, Chief, Protective Structures Branch. Dr. J. D. Smart, R. G. Dodson, and D. G. Heitmann participated in the monitoring work.

TABLE OF CONTENTS

	Page
Abstract	ii
Preface	iii
Introduction.	1
Dimensional Analysis	1
Scaling of Field Measurements from Contained Explosions	6
Estimation of Direct Induced Motions from Surface Bursts on Rock	9
Tables.	13
Figures	21
References	26

LIST OF TABLES

TABLE		Page
I	Variables Considered in Dimensional Analysis of Explosion Phenomena	13
II	Events from Which Ground Motion Data Were Obtained and Scaled.	14
III	Ground Motion Data (Hardhat, H.E. Sandstone, Ranier, Gnome, Shoal, Dugout).	15
IV	Ground Motion Data (Longshot).	19
V	Ground Motion Data (Piledriver, Gas Buggy)	20

LIST OF FIGURES

Figure		Page
1	Typical Wave Form for Direct-Transmitted Ground Shock	21
2	Data Plots Suggested by Dimensional Analysis . . .	22
3	Variation of Strain with Range for Contained Bursts	23
4	Scaled Acceleration versus Scaled Range for Contained Bursts	24
5	Definition of Radius Orientation	25

CONVERSION FACTORS, BRITISH TO METRIC UNITS OF MEASUREMENT

British units of measurement used in this report can be converted to metric units as follows:

<u>Multiply</u>	<u>By</u>	<u>To Obtain</u>
inches	2.54	centimeters
feet	0.3048	meters
cubic inches	16.3871	cubic centimeters
pounds	0.45359237	kilograms
pounds per square inch	0.070307	kilograms per square centimeter
pounds per cubic foot	16.0185	kilograms per cubic meter
inch-pounds	0.011521	Meter-kilograms
inches per second	2.54	centimeters per second
inches per second per second	2.54	centimeters per second per second

Introduction

The design of close in protective structures in rock requires the estimation of the ground motions from direct ground shock. At present, the magnitude of these motions is best estimated by scaling the field measurements from fully contained nuclear detonations. The fully contained data are then adjusted by means of a "coupling" factor to apply to the surface burst case considered for design.

In this report, the concepts of scaling are discussed and field measurements from underground explosions are scaled according to the principles developed. Recommendations are also given for extrapolation of the contained data to estimate motions in a rock medium below a surface burst.

Dimensional Analysis

The empirical scaling of shock phenomena from explosions involves the comparison of dynamic measurements obtained at various distances in different media from a wide range of yields. Quite often scaling is used to estimate ground motions by extrapolation to yields which are far beyond the range of yields from which the experimental data were obtained. For these cases, it is very important that the scaling relation be guided by dimensional analysis such that the empirical relations obtained are dimensionally homogeneous. It is also important that certain relations exist among empirical equations for maximum acceleration, particle velocity, and displacement such that the equations are kinematically consistent. In this section, principles are developed for formulating empirical equations for ground motions from experimental data which are kinematically admissible and which are dimensionally homogeneous.

The dependent variables considered in such an analysis are the displacement δ , the particle velocity v , and the acceleration a , which result at some point due to the explosion. The independent variables considered the most significant in influencing the ground motions are the energy released by the detonation W , the range from the detonation to the point of observation R , the density of the rock ρ , the compressional seismic velocity in the rock mass c , and time t . Table I gives dimensions of all variables considered in terms of force F , length L , and time T .

According to the Buckingham Pi theorem (Murphy, 1950), the dependent variables are related to dimensionless groups of the independent variables as follows:

$$\frac{\delta}{R} = g_1 \left[\frac{tc}{R}, \frac{W}{\rho c^2 R^3} \right] \quad (1)$$

$$\frac{v}{c} = g_2 \left[\frac{tc}{R}, \frac{W}{\rho c^2 R^3} \right] \quad (2)$$

$$\frac{aR}{c^2} = g_3 \left[\frac{tc}{R}, \frac{W}{\rho c^2 R^3} \right] \quad (3)$$

where g_1 , g_2 , and g_3 are unknown functions of the dimensionless groups of independent variables (Pi terms).

If the maximum values of displacement, particle velocity, and acceleration are of interest, the Pi term tc/R is usually neglected because this term relates only to the time scaling of the phenomena. It is interesting to note however, that R/c is the transit time of a pulse from the point of detonation to a point at a distance R . Thus, the Pi term tc/R indicates that "times" (rise time, duration time, etc.) describing the character of

the pulse should scale directly proportional to the transit time. Figure 1 shows a typical qualitative wave form produced by shock directly transmitted into rock by explosions. In general, available data indicate that the rise time to peak particle velocity t_r , as shown on Figure 1, is 1/6 to 1/12 the transit time of the pulse (Newmark and Halmiwanger, 1962). The positive phase duration of the velocity pulse t_d which corresponds to the time of maximum displacement is roughly 1 to 2 times the transit time as illustrated in Figure 1. Thus, the available field data appear to support that "times" scale proportional to the transit times as indicated in Eqs. 1 through 3. Thus, if maximum values of δ , v , and a occur at constant values of tc/R , or if tc/R is not important in determining the maximum values of δ , v , and a , then the dimensionless maximum displacement, velocity, and acceleration are given as functions g_δ , g_v , and g_a of only the dimensionless variable $W/\rho c^2 R^3$ as given below.

$$\frac{\delta}{R} = g_\delta \left(\frac{W}{\rho c^2 R^3} \right) \quad (4)$$

$$\frac{v}{c} = g_v \left(\frac{W}{\rho c^2 R^3} \right) \quad (5)$$

$$\frac{aR}{c^2} = g_a \left(\frac{W}{\rho c^2 R^3} \right) \quad (6)$$

Thus, according to the dimensional analysis presented, the field measurements of maximum acceleration, velocity, and displacement at various ranges from different yield detonations in different media should be plotted as shown in Figure 2. If the scaling described works, then the data should collapse along a given curve in the plots shown in Fig. 2 and should enable the functions g_δ , g_v , and g_a to be determined.

Normally, the plots suggested in Figure 2 are made on log-log paper and much of the relationship of interest can be approximated by a straight line. Thus, the equations for δ , v , and a are of the form:

$$\frac{\delta}{R} = K \left[R \left(\frac{\rho c^2}{W} \right)^{1/3} \right]^{n_\delta} \quad (7)$$

$$\frac{v}{c} = K_1 \left[R \left(\frac{\rho c^2}{W} \right)^{1/3} \right]^{n_v} \quad (8)$$

$$\frac{aR}{c^2} = K_2 \left[R \left(\frac{\rho c^2}{W} \right)^{1/3} \right]^{n_a} \quad (9)$$

Thus:

$$\delta = K R^{n_\delta+1} \left(\frac{\rho}{W} \right)^{n_\delta/3} c^{2/3 n_\delta} \quad (10)$$

$$v = K_1 R^{n_v} \left(\frac{\rho}{W} \right)^{n_v/3} c^{2/3 n_v+1} \quad (11)$$

$$a = K_2 R^{n_a-1} \left(\frac{\rho}{W} \right)^{n_a/3} c^{2/3 n_a+2} \quad (12)$$

According to dimensional analysis, the exponents n_δ , n_v , and n_a in Eqs. 7, 8, and 9 need not be related; but since the maximum values of displacement, velocity, and acceleration are kinematically related, then realistic constraints must be investigated which are necessary to make these quantities kinematically consistent. For example, from Fig. 1 it is apparent that the maximum acceleration, a_{\max} , is given by

$$a_{\max} = K_3 \frac{v_{\max}}{t_r} \quad (13)$$

and that

$$\delta_{\max} = K_4 v_{\max} \cdot t_d \quad (14)$$

where K_3 and K_4 depend on the shape of the pulse. For a given shape pulse the rise time, t_r , is also given by

$$t_r = K_5 t_d \quad (15)$$

Thus, substitution of Eq. 15 into Eq. 13 and multiplication of Eqs. 13 and 14 yields

$$a_{\max} \cdot \delta_{\max} = \frac{K_3 K_4}{K_5} v_{\max}^2 \quad (16)$$

Newmark (1968) has shown that the constant $K_3 K_4/K_5$ is always less than 0.5. Nevertheless, Eq. 16 shows that, independent of the value of $K_3 K_4/K_5$, Eqs. 7, 8, and 9 should satisfy the relationship

$$2n_v = n_\delta + n_a \quad (17)$$

in order for Eq. 16 to be satisfied.

For example, say that it was found that $n_v = -2$ and $n_a = -2$ from experiments. For Eq. 17, n_δ would also have to be -2. Equations 10, 11, and 12 then would be of the form

$$\delta = K R^{-1} \frac{W^{2/3}}{\rho} c^{-4/3} \quad (18)$$

$$v = K_1 R^{-2} \frac{W^{2/3}}{\rho} c^{-1/3} \quad (19)$$

$$a = K_2 R^{-3} \frac{W^{2/3}}{\rho} c^{+2/3} \quad (20)$$

in order to be kinematically consistent.

Scaling of Field Measurements from Contained Explosions

Radial accelerations and particle velocities from the contained explosions given in Table II are given in Tables III, IV, and V. The data presented in Tables III - V are shown scaled in the manner suggested in Fig. 2 and plotted in Figs. 3, and 4. Some of the data given are from HE experiments and some are from nuclear experiments. It should be noted that no adjustment has been made for the relative efficiency of nuclear and HE contained bursts for the scaled points shown in Figs. 3 and 4. If there is a difference in efficiency between HE and nuclear contained bursts in producing direct ground shock, then the difference appears to be small enough to be masked by the normal scatter in ground motion data. The relative position of the UET sandstone data and the Gas Buggy sandstone data in Fig. 3 tend to illustrate the point that there is no discernible difference in efficiency which could be detected within the scatter of the data. From Figs. 3 and 4, the best fit to the data indicates that n_v and $n_a = -2.5$. Thus, the form of the scaling relation suggested is

$$\frac{v}{c} = K_1 \left[(R) \left(\frac{\rho c^2}{W} \right)^{1/3} \right]^{-5/2} \quad (21)$$

$$\frac{aR}{c^2} = K_2 \left[(R) \left(\frac{\rho c^2}{W} \right)^{1/3} \right]^{-5/2} \quad (22)$$

Since

$$n_\delta = 2n_v - n_a \quad (23)$$

then a consistent relationship for the maximum dynamic displacement should be of the form:

$$\frac{\delta}{R} = K \left[(R) \left(\frac{\rho c^2}{W} \right)^{1/3} \right]^{-5/2} \quad (24)$$

Thus a set of consistent equations should be of the form:

$$\epsilon = \frac{v}{c} = K_1 W^{5/6} \rho^{-5/6} c^{-5/3} R^{-5/2} \quad (25)$$

$$v = K_1 W^{5/6} \rho^{-5/6} c^{-2/3} R^{-5/2} \quad (26)$$

$$a = K_2 W^{5/6} \rho^{-5/6} c^{+1/3} R^{-7/2} \quad (27)$$

$$\delta = K W^{5/6} \rho^{-5/6} c^{-5/3} R^{-3/2} \quad (28)$$

Evaluation of the constants K_1 and K_2 from the data presented in Figs. 3 and 4 yield equations for maximum radial strain, maximum radial acceleration and maximum radial particle velocity as follows for fully contained nuclear detonations

$$\epsilon_r = \frac{v}{c} = 0.0015 \left(\frac{W}{50 \text{ Kt}} \right)^{5/6} \left(\frac{1000 \text{ ft}}{R} \right)^{5/2} \left(\frac{165 \text{ pcf}}{\gamma} \right)^{5/6} \left(\frac{18,000 \text{ fps}}{c} \right)^{5/3} \quad (29)$$

$$a = 180 \text{ g} \left(\frac{W}{50 \text{ Kt}} \right)^{5/6} \left(\frac{1000 \text{ ft}}{R} \right)^{7/2} \left(\frac{165 \text{ pcf}}{\gamma} \right)^{5/6} \left(\frac{c}{18,000 \text{ fps}} \right)^{1/3} \quad (30)$$

$$v_r = \epsilon_r \cdot c = 27 \text{ fps} \left(\frac{W}{50 \text{ Kt}} \right)^{5/6} \left(\frac{1000 \text{ ft}}{R} \right)^{5/2} \left(\frac{165 \text{ pcf}}{\gamma} \right)^{5/6} \left(\frac{18,000 \text{ fps}}{c} \right)^{2/3} \quad (31)$$

The maximum radial stress, σ_r , is given by

$$\sigma_r = \rho v_r c_p \quad (32)$$

where c_p is the propagation velocity of the peak radial stresses. In the Climax Stock Granite (location of the Pile Driver, Hardhat, Shoal, and Tiny Tot tests) the propagation of the peak stresses in the close in ranges was about 14,000 ft/sec, and the seismic velocity was about 18,000 ft/sec. Then by Eqs. 31 and 32, the radial stress at a range of 1000 ft in a medium with a seismic velocity, c , of 18,000 ft/sec would be given by

$$\sigma_r = (27 \text{ ft/sec})(14,000 \text{ ft/sec}) \left(\frac{165 \text{ lb/ft}^3}{32.2 \text{ ft/sec}^2} \right) \left(\frac{1 \text{ psi}}{144 \text{ lb/ft}^2} \right) = 13,500 \text{ psi}$$

and a general equation for radial stress would be given by

$$\sigma_r = 13,500 \text{ psi} \left[\frac{W}{50 \text{ Kt}} \right]^{5/6} \left[\frac{1000 \text{ ft}}{R} \right]^{5/2} \left[\frac{\gamma}{165 \text{ pcf}} \right]^{1/6} \left[\frac{c}{18,000 \text{ fps}} \right]^{1/3} \quad (33)$$

where c is the seismic velocity of the medium. Equation 33 is a reasonable approximation for the radial stresses when the peak stress propagation velocity, c_p , is about $\left(\frac{14,000 \text{ ft/sec}}{18,000 \text{ ft/sec}} = 0.78 \right)$ 0.80 times the seismic velocity of the medium. For those cases where c_p/c is different than 0.80, the value obtained from Eq. 33 should be multiplied by

$$\left(\frac{c_p/c}{0.8} \right)$$

If the positive duration t_d of the velocity pulse is approximately 1 to 2 times the transit time, R/c , then for 1000 ft from 50 Kt in a medium with a unit weight of 165 pcf and a seismic velocity of 18,000 fps the

maximum displacement for a nearly triangular pulse as shown in Fig. 1 would be:

$$\delta_{\max} = 1/2 v_{\max} \cdot t_d \quad (34)$$

and K would range from

$$1/2 \times 27 \text{ ft/sec} \times \frac{1000 \text{ ft}}{18,000 \text{ ft/sec}} \times 1 = 0.75 \text{ ft}$$

to

$$1/2 \times 27 \text{ ft/sec} \times \frac{1000 \text{ ft}}{18,000 \text{ ft/sec}} \times 2 = 1.5 \text{ ft}$$

and the equation for maximum radial displacement would be

$$\delta = 1.5 \text{ ft} \left(\frac{W}{50 \text{ Kt}} \right)^{5/6} \left(\frac{1000 \text{ ft}}{R} \right)^{3/2} \left(\frac{165 \text{ pcf}}{\gamma} \right)^{5/6} \left(\frac{18,000 \text{ ft/sec}}{c} \right)^{5/3} \quad (35)$$

for a fully contained burst.

Estimation of Direct Induced Motions from Surface Bursts on Rock

To estimate deep underground motions, engineers have used the concept of an effective or equivalent yield, W_e . The equivalent yield is defined as the yield of a contained nuclear explosion that would provide the observed peak stress, strain, or particle velocity at a given range beneath ground zero of a nuclear surface burst of yield W_s . The ratio W_e/W_s is then defined as an effective coupling factor. Based on peak particle velocity data from low yield nuclear detonations in underground cavities in granite and tuff, an equivalent yield coupling factor of about 10 to 12 percent would be inferred. Cooper, Brode, and Leigh (1971) have stated that the "coupling"

factors obtained from the low yield cavity experiments are probably too high to be used for the case of large yield surface bursts because the more massive (low yield to mass ratio) low yield devices are expected to couple energy to the ground more efficiently than the large yield devices. Thus, the most current estimate of the coupling factor for peak velocities, strains, stresses, and accelerations is about 5 percent for motions directly beneath a large yield surface burst on a rock medium (Cooper, Brode, and Leigh, 1971). An equivalent yield or "coupling" factor however, would be expected to be lower for peak particle displacements than for peak particle velocities because free surface effects reduce the positive phase duration of the particle velocity pulse from that which would be observed in a fully-tamped burst. A study of the data for the low yield cavity experiments, (Cooper, 1971), does indeed indicate that the coupling factor for peak displacements could be about one-third to two-thirds the coupling factor for peak particle velocities. Thus, it is felt that it would be conservative to use a coupling factor of about 3 percent for estimating peak radial displacements below a large yield surface burst on rock. Thus, for 5 percent coupling, the best estimate for direct induced radial accelerations, particle velocities, stresses and strains directly below a surface burst on rock are given by:

$$a_r = 180 g \left(\frac{W_s}{1 \text{ MT}} \right)^{5/6} \left(\frac{1000 \text{ ft}}{R} \right)^{7/2} \left(\frac{165 \text{ pcf}}{\gamma} \right)^{5/6} \left(\frac{c}{18,000 \text{ fps}} \right)^{1/3} \quad (36)$$

$$v_r = 27 \text{ fps} \left(\frac{W_s}{1 \text{ MT}} \right)^{5/6} \left(\frac{1000 \text{ ft}}{R} \right)^{5/2} \left(\frac{165 \text{ pcf}}{\gamma} \right)^{5/6} \left(\frac{18,000 \text{ fps}}{c} \right)^{2/3} \quad (37)$$

$$\epsilon_r = 0.0015 \left(\frac{W_s}{1 \text{ MT}} \right)^{5/6} \left(\frac{1000 \text{ ft}}{R} \right)^{5/2} \left(\frac{165 \text{ pcf}}{\gamma} \right)^{5/6} \left(\frac{18,000 \text{ fps}}{c} \right)^{5/3} \quad (38)$$

$$\sigma_r = 13,500 \text{ psi} \left(\frac{W}{1 \text{ MT}} \right)^{5/3} \left(\frac{1000 \text{ ft}}{R} \right)^{5/2} \left(\frac{\gamma}{165 \text{ pcf}} \right)^{1/6} \left(\frac{c}{18,000 \text{ fps}} \right)^{1/3} \quad (39)$$

If a 3 percent coupling factor is used for estimating peak radial displacements, then Eq. 35 may be altered to apply to the surface burst case to yield

$$\delta_r = 1 \text{ ft} \left(\frac{W}{1 \text{ MT}} \right)^{5/6} \left(\frac{1000 \text{ ft}}{R} \right)^{3/2} \left(\frac{165 \text{ pcf}}{\gamma} \right)^{5/6} \left(\frac{18,000 \text{ fps}}{c} \right)^{5/3} \quad (40)$$

Equations 36, 37, 38, 39 and 40 are applicable for estimating radial motions along a vertical radius extending below the center of the crater of a surface burst, i.e., $\theta = 0^\circ$ Fig. 5. For motion predictions along radii for $\theta < 70^\circ$, Fig. 5, theoretical studies (Cooper, Brode, and Leigh, 1971) indicate that Eqs. 36, 37 and 38 can be multiplied by a correction factor F_θ to give reduced motions along radii at $\theta > 0^\circ$. The value of F_θ suggested by Cooper, Brode, and Leigh (1971) is given by

$$F_\theta = (\cos \theta + 0.1 \sin \theta) \quad (41)$$

where θ is defined in Fig. 5. Since Eq. 41 is based on highly complex computational models (Trullo, 1970), and the results for values of θ greater than 60° are very sensitive to the unloading properties assumed for the medium, it is felt at this time that a value of F_θ should be used for design which is more conservative than the value given by Eq. 41. The following correction value is suggested.

$$F_\theta = 0.5 (1 + \cos \theta) \quad (42)$$

Equation 42 can be applied to Eq. 40 for displacements for values of θ up to 65° , but cannot be used for values of $\theta > 65^\circ$ because particle displacements at shallow depths from cratering effects are not predictable by using the seismic velocity as the pertinent property of the medium. The prediction of crater induced motions at shallow depths has been treated elsewhere (Cooper, Brode and Leigh, 1971). It should also be pointed out that Eqs. 36, 37, 38, 39 and 40 should not be used for media with seismic velocities less than about 9000 ft/sec because the tuff data ($c = 6000$ fps) shown in Figs. 3 and 4 does not correlate with the data upon which these equations are based.

It should also be noted that, at this time, the equations developed herein should not be modified for use in design cases where the rock medium in question is saturated and below the water table. Much of the data included in this analysis has been from rock masses which were saturated and the data already inherently includes the effects of porepressures if they are significant. This is especially true of the Long Shot data obtained on Amchitka Island. Field information also indicates that the tuff and granite formations at Nevada Test Site are essentially saturated at the depths at which information has been obtained and the sandstone formation from which the Gas Buggy data were obtained was also saturated.

TABLE I

Variables Considered in Dimensional Analysis
of Explosion Phenomena

Variable	Symbol	Dimension
(Independent Variables)		
Energy Released by Explosion	W	FL
Distance from Explosion (Range)	R	L
Seismic Velocity of Rock Mass	c	LT^{-1}
Density of the Rock Mass	ρ	$FT^2 L^{-4}$
Time	t	T
(Dependent Variables)		
Displacement	δ	L
Particle Velocity	v	LT^{-1}
Acceleration	a	LT^{-2}

TABLE II

Events from Which Ground Motion Data Were
Obtained and Scaled

Event	Medium
Hardhat	Granite
Shoal	Granite
Piledriver	Granite
Longshot	Andesite
Gnome	Salt
Rainier	Tuff
Dugout	Basalt
Underground Explosion Tests	Sandstone
Gas Buggy	Sandstone

TABLE III

Shot Matl.	W	ρ	c	v	$\frac{v}{c}$	a	$\frac{aR}{c^2}$	R	$R(\frac{\rho c^2}{W})^{1/3}$
	#TNT or Kilotons	Slug Ft ³	$\frac{Ft}{Sec}$	$\frac{Ft}{Sec}$	-	$\frac{Ft}{Sec^2}$	-	Ft	$(\frac{Ft \cdot lb}{Kc})^{1/3}$
Hardhat (Nucl.)	5.9 Kt	4.97	18000	57	3.16×10^{-3}	1.35×10^5	1.12×10^{-1}	270	1.75×10^5
	"	"	"	61	3.39×10^{-3}	6.3×10^4	6.01×10^{-2}	310	2.00×10^5
	"	"	"	30	1.67×10^{-3}	1.55×10^4	1.96×10^{-2}	410	2.66×10^5
Granite	"	"	"	21	1.17×10^{-3}	6.75×10^3	1.06×10^{-2}	510	3.32×10^5
	"	"	"	11	6.10×10^{-4}	1.35×10^3	2.54×10^{-3}	610	3.96×10^5
	"	"	"	7.2	4×10^{-4}	1.03×10^3	2.68×10^{-3}	800	5.19×10^5
	"	"	"	5.5	3.05×10^{-4}			800	5.19×10^5
	"	"	"	3.7	2.06×10^{-4}	2.58×10^2	1.19×10^{-3}	1500	9.72×10^5
	"	"	"	2.4	1.33×10^{-4}			"	9.72×10^5
	"	"	"	1.7	9.43×10^{-5}			"	9.72×10^5
320 lb. (H.E.)	4.5	9000		6.8	7.58×10^{-4}			24.6	3.36×10^5
	"	"	"	4.5	5×10^{-4}			34	4.45×10^5
	"	"	"	.4	4.44×10^{-5}			99.8	1.31×10^6
Sand- stone	"	"	"	4.6	5.11×10^{-4}			26.2	3.43×10^5
	"	"	"	1.2	1.33×10^{-4}			41.2	5.40×10^5
	"	"	"	.3	3.34×10^{-5}			101.9	1.34×10^6
1080	"	"	"	1.1	1.21×10^{-4}			74	6.50×10^5
"	"	"	"	.1	1.11×10^{-5}			157.5	1.39×10^6
2560	"	"	"	20.6	2.29×10^{-3}			56	3.70×10^5
"	"	"	"	10.6	1.18×10^{-3}			56	3.70×10^5
"	"	"	"	.2	2.22×10^{-5}			229	1.51×10^6

TABLE III (continued)

S. no.	Matl.	W	ρ	C	V	$\frac{V}{C}$	a	$\frac{aR}{C^2}$	R	$R(\frac{\rho C}{W})^{1/3}$
	#TNT or Kilotons	Slug Ft ³	$\frac{Ft}{Sec}$	$\frac{Ft}{Sec}$	$\frac{Ft}{Sec}$	-	$\frac{Ft}{Sec^2}$	-	Ft	$(\frac{Ft \cdot lb}{Kt})^{1/3}$
Ranier (Nucl.)	1.7 Kt	2.72	7000	17.5	2.5×10^{-3}				175	7.50×10^4
	"	"	"	7.3	1.04×10^{-3}				200	8.56×10^4
	"	"	"	4.0	5.72×10^{-4}				350	1.50×10^5
	"	"	"	2.2	3.14×10^{-4}				540	2.32×10^5
	"	"	"	1.45	2.07×10^{-4}				740	3.18×10^5
Gnome (Nucl.)	3 Kt	4.92	13,400	230	1.72×10^{-2}		3.28×10^5	3.65×10^{-1}	200	1.33×10^5
	"	"	"	80	5.96×10^{-3}		8.05×10^4	1.12×10^{-1}	250	1.66×10^5
	"	"	"	100	7.46×10^{-3}		1.22×10^5	1.70×10^{-1}	250	1.66×10^5
	"	"	"	40	2.99×10^{-3}		2.48×10^4	4.43×10^{-2}	320	2.13×10^5
	"	"	"	130	9.70×10^{-3}				320	2.13×10^5
Salt	"	"	"	30	2.24×10^{-3}		1.03×10^4	2.30×10^{-2}	400	2.67×10^5
	"	"	"	32	2.39×10^{-3}		1.10×10^4	2.45×10^{-2}	"	2.67×10^5
	"	"	"	33	2.46×10^{-3}				"	2.67×10^5
	"	"	"	35	2.61×10^{-3}				"	2.67×10^5
	"	"	"	14	1.04×10^{-3}		4.51×10^3	1.43×10^{-2}	570	3.30×10^5
	"	"	"	30	2.24×10^{-3}				"	3.80×10^5
	"	"	"	13	9.70×10^{-4}		1.93×10^3	8.29×10^{-3}	770	5.14×10^5
	"	"	"	15	1.12×10^{-3}		1.42×10^3	6.08×10^{-3}	"	5.14×10^5
	"	"	"	10	7.46×10^{-4}		8.05×10^2	4.48×10^{-3}	1000	6.66×10^5
	"	"	"	3	2.24×10^{-4}		2.25×10^2	1.87×10^{-3}	1500	1.00×10^6
	"	"	"	7	5.22×10^{-4}				1000	6.66×10^5
	"	"	"	9	6.71×10^{-4}				1000	6.66×10^5

TABLE III (continued)

Shot Matl.	W	ρ	C	V	$\frac{V}{C}$	a	$\frac{aR}{C^2}$	R	$R(\frac{\rho C}{W})^{1/3}$
	#TNT or Kilotons	Slug Ft ³	$\frac{Ft}{Sec}$	$\frac{Ft}{Sec}$	-	$\frac{Ft}{Sec^2}$	-	Ft	$(\frac{Ft \cdot lb}{Kt})^{1/3}$
Shoal (NucI.)	12.5 Kt	4.97	18000	220	1.22×10^{-2}	17.5×10^4	1.64×10^{-1}	303	1.52×10^5
	"	"	"	49	2.72×10^{-3}	9.01×10^3	1.39×10^{-2}	500	2.52×10^5
	"	"	"	11.6	6.44×10^{-4}	1.93×10^3	4.94×10^{-3}	831	4.17×10^5
Granite	"	"	"	5.1	2.83×10^{-4}	5.47×10^2	2.19×10^{-3}	1301	6.58×10^5
	"	"	"	1.45	8.05×10^{-5}	1.35×10^2	8.00×10^{-4}	1924	9.71×10^5
	"	"	"	2.35	1.36×10^{-4}	1.21×10^2	7.23×10^{-4}	1939	9.77×10^5
	"	"	"	1.82	1.01×10^{-4}	1.45×10^2	8.72×10^{-4}	1953	9.84×10^5
Dugout (H.E.)	40×10^3 lb	5	1.07×10^4	214	2×10^{-2}	7.15×10^5	2.81×10^{-1}	45	1.37×10^5
	"	5	9.18×10^3	38.5	4.19×10^{-3}	1.76×10^4	1.88×10^{-2}	90	2.48×10^5
	"	5	8.25×10^3	7.1	8.6×10^{-4}	1.93×10^3	3.83×10^{-3}	135	3.48×10^5
Basalt	"	5	7.06×10^3	4.5	6.38×10^{-4}	1.06×10^3	3.82×10^{-3}	180	4.17×10^5
	"	5	6.14×10^3	1.7	2.77×10^{-4}	2.90×10^2	1.73×10^{-3}	225	4.76×10^5
(H.E.)	320 lb	4.5	9000			10.3×10^4	2.88×10^{-2}	22.6	2.96×10^5
	320 lb	4.5	9000			4.9×10^3	3.45×10^{-3}	54.8	7.19×10^5
Sand-	2560 lb	4.5	9000			15.3	2.55×10^{-4}	274	1.80×10^6
stone	40×10^3 lb	4.5	9000			14.1	8.92×10^{-5}	513	1.35×10^6

TABLE IV

Shot Material	W	ρ	c	v	$\frac{v}{c}$	a	$\frac{aR}{c^2}$	R	$R(\frac{\rho c^2}{W})^{1/3}$
Long Shot	Kt	$\frac{\text{Slug}}{\text{Ft}^3}$	$\frac{\text{Ft}}{\text{Sec}}$	$\frac{\text{Ft}}{\text{Sec}}$	-	$\frac{\text{Ft}}{\text{Sec}^2}$	-	Ft	$(\frac{\text{Ft} \cdot \text{lb}}{\text{Kt}})^{1/3}$
Andesite									
"	1*	4.66	11,000	15.6	1.42×10^{-3}	3330	1.15×10^{-2}	419	3.5×10^5
"	"	"	"	18.2	1.66×10^{-3}	3100	9×10^{-2}	372	3.1×10^5
"	"	"	"	25.8	2.34×10^{-3}	5680	1.53×10^{-2}	326	2.7×10^5
"	"	"	"	28.8	2.62×10^{-3}	6940	1.59×10^{-2}	279	2.3×10^5

* All data and distances scaled by cube root scaling to 1 Kt.

TABLE V

Shot Material	W	ρ	C	V	$\frac{V}{C}$	a	$\frac{aR}{C^2}$	R	$R(\frac{\rho C}{W})^{1/3}$
Piledriver	Kt	$\frac{\text{Slug}}{\text{Ft}^3}$	$\frac{\text{Ft}}{\text{Sec}}$	$\frac{\text{Ft}}{\text{Sec}}$	-	$\frac{\text{Ft}}{\text{Sec}^2}$	-	Ft	$(\frac{\text{Ft} \cdot \text{lb}}{\text{Kt}})^{1/3}$
"	1*	5.12	18,000	110	6.1×10^{-3}			170	2.02×10^5
"	"	"	"	98	5.4×10^{-3}			150	1.78×10^5
"	"	"	"	50	2.8×10^{-3}	4.20×10^4	2.78×10^{-2}	215	2.55×10^5
"	"	"	"	38	2.1×10^{-3}			240	2.84×10^5
"	"	"	"	38	2.1×10^{-3}	1.77×10^4	1.42×10^{-2}	260	3.08×10^5
"	"	"	"	27	1.5×10^{-3}	1.77×10^4	1.37×10^{-2}	250	2.96×10^5
"	"	"	"	21	1.2×10^{-3}			240	2.84×10^5
"	"	"	"	19	1.0×10^{-3}	$.61 \times 10^4$	7.6×10^{-3}	400	4.74×10^5
"	"	"	"	13	7.2×10^{-4}			400	4.74×10^5
"	"	"	"	9.1	5.0×10^{-4}			520	6.16×10^5
"	"	"	"	6.3	3.5×10^{-4}			540	6.40×10^5
"	"	"	"	6.0	3.3×10^{-4}			520	6.16×10^5
"	"	"	"	6.0	3.3×10^{-4}			760	9.0×10^5
"	"	"	"	3.8	2.1×10^{-4}			750	8.9×10^5
Gas Buggy									
Sandstone	29	4.5	15,000	4.35	2.9×10^{-4}			1820	5.8×10^5
"	"	"	"	5.18	3.5×10^{-4}			1665	5.3×10^5
"	"	"	"	7.80	5.2×10^{-4}			1530	4.9×10^5
"	"	"	"	6.50	4.3×10^{-4}			1565	5.0×10^5

* All data and distances scaled by cube root scaling to 1 Kt.

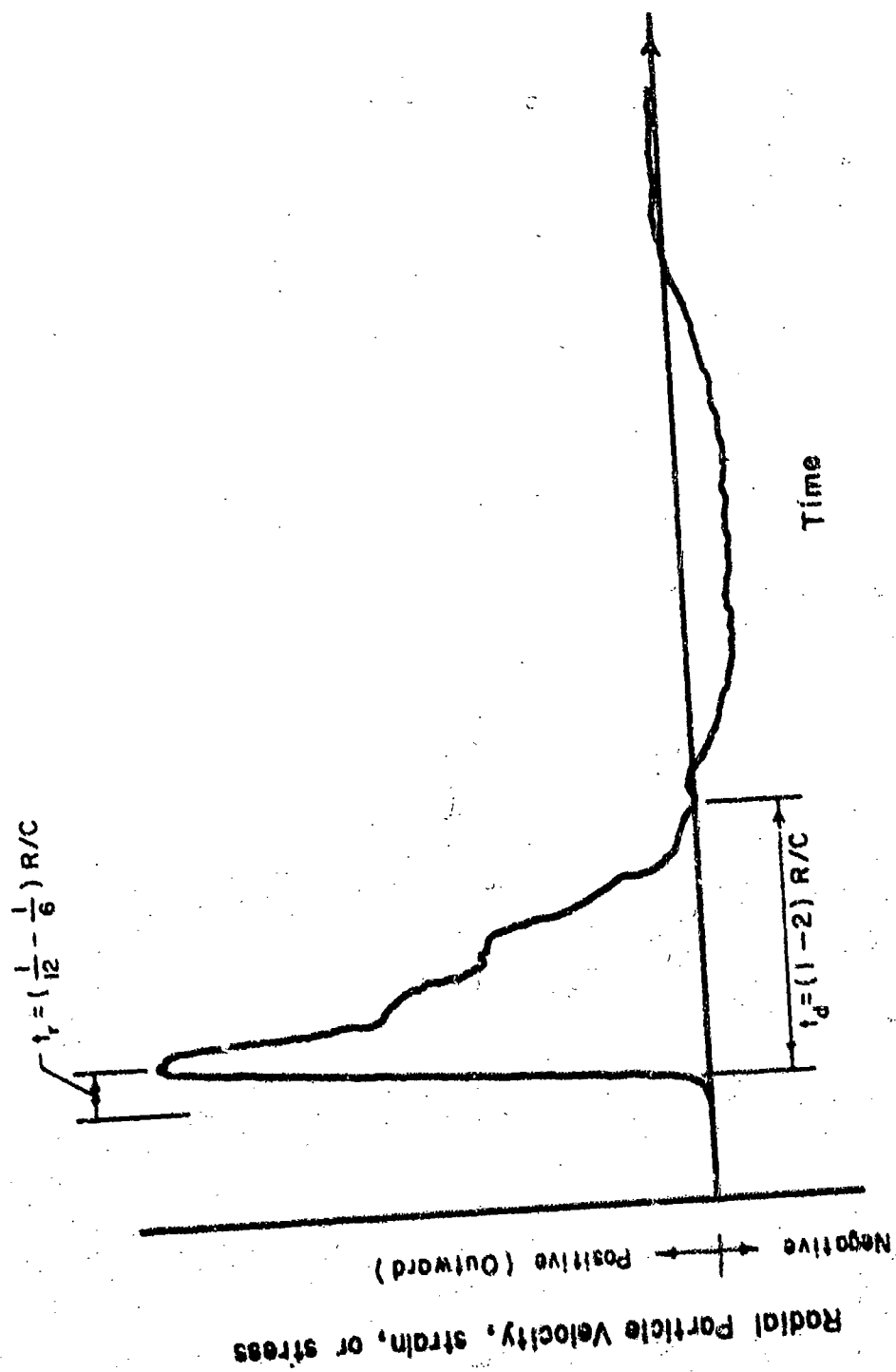
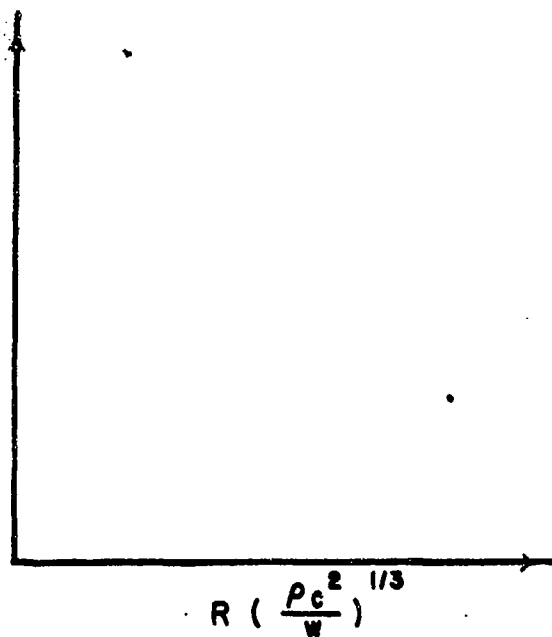
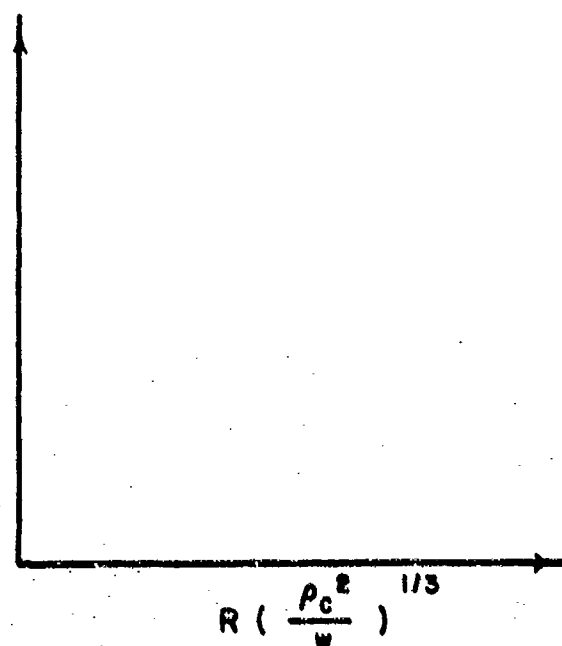


FIG. 1 TYPICAL WAVE FORM FOR DIRECT-TRANSMITTED GROUND SHOCK

$$e = v/c$$



$$\frac{\partial R}{c^2}$$



$$\delta/R$$

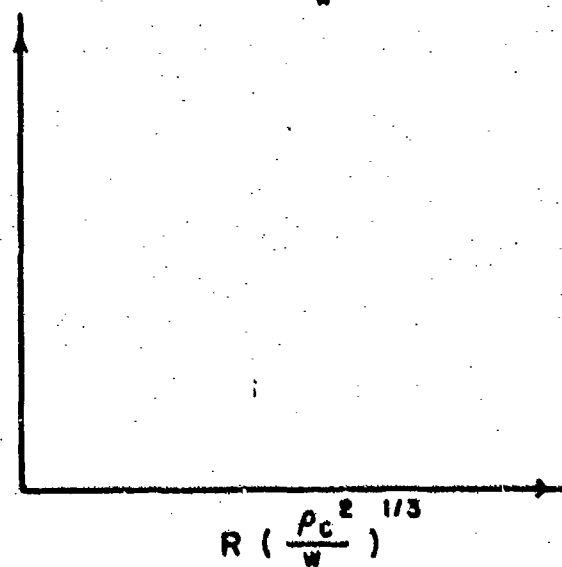


FIG. 2 DATA PLOT SUGGESTED BY DIMENSIONAL ANALYSIS

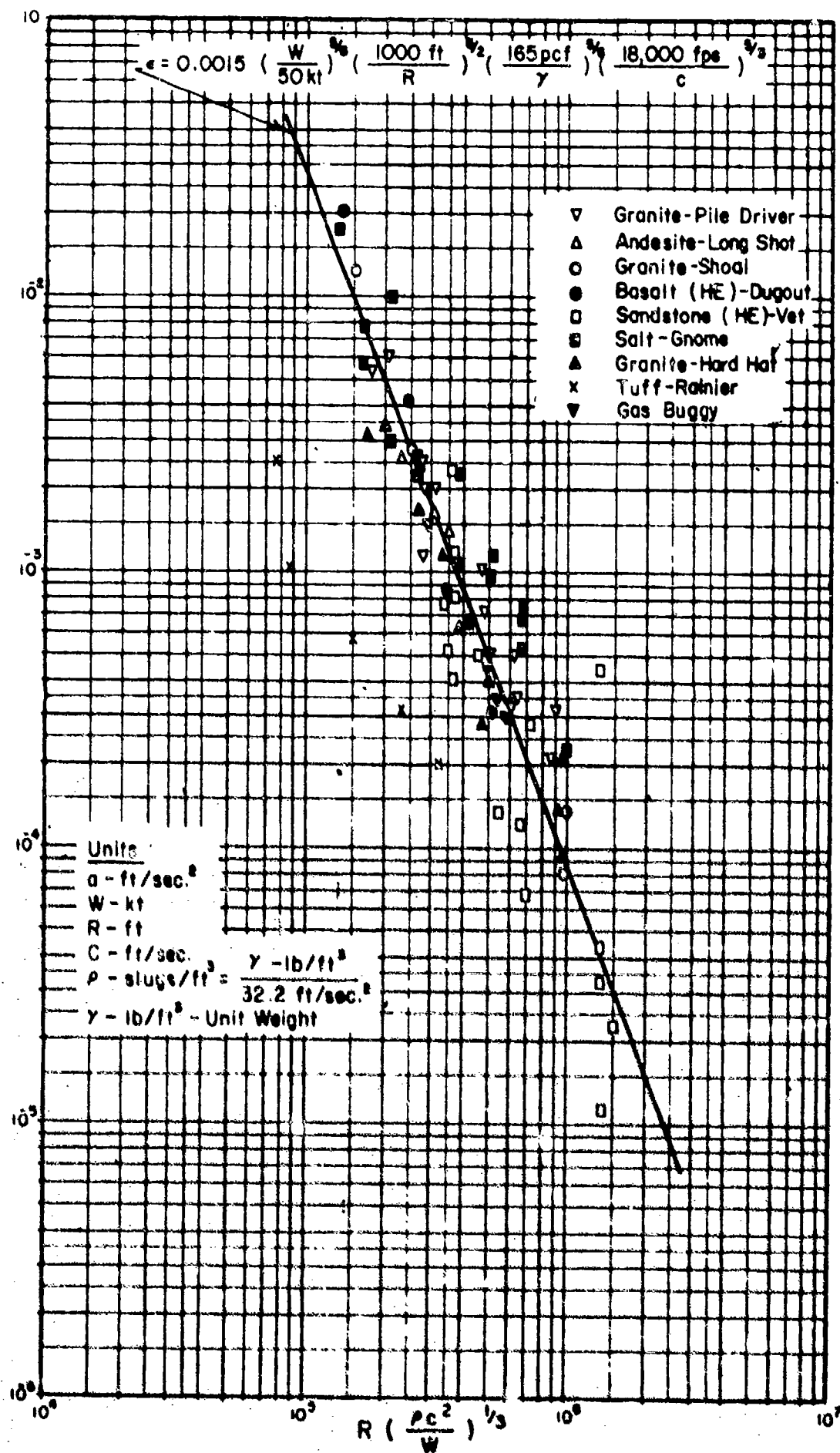


FIG. 3 VARIATION OF STRAIN WITH RANGE FOR CONTAINED BURSTS

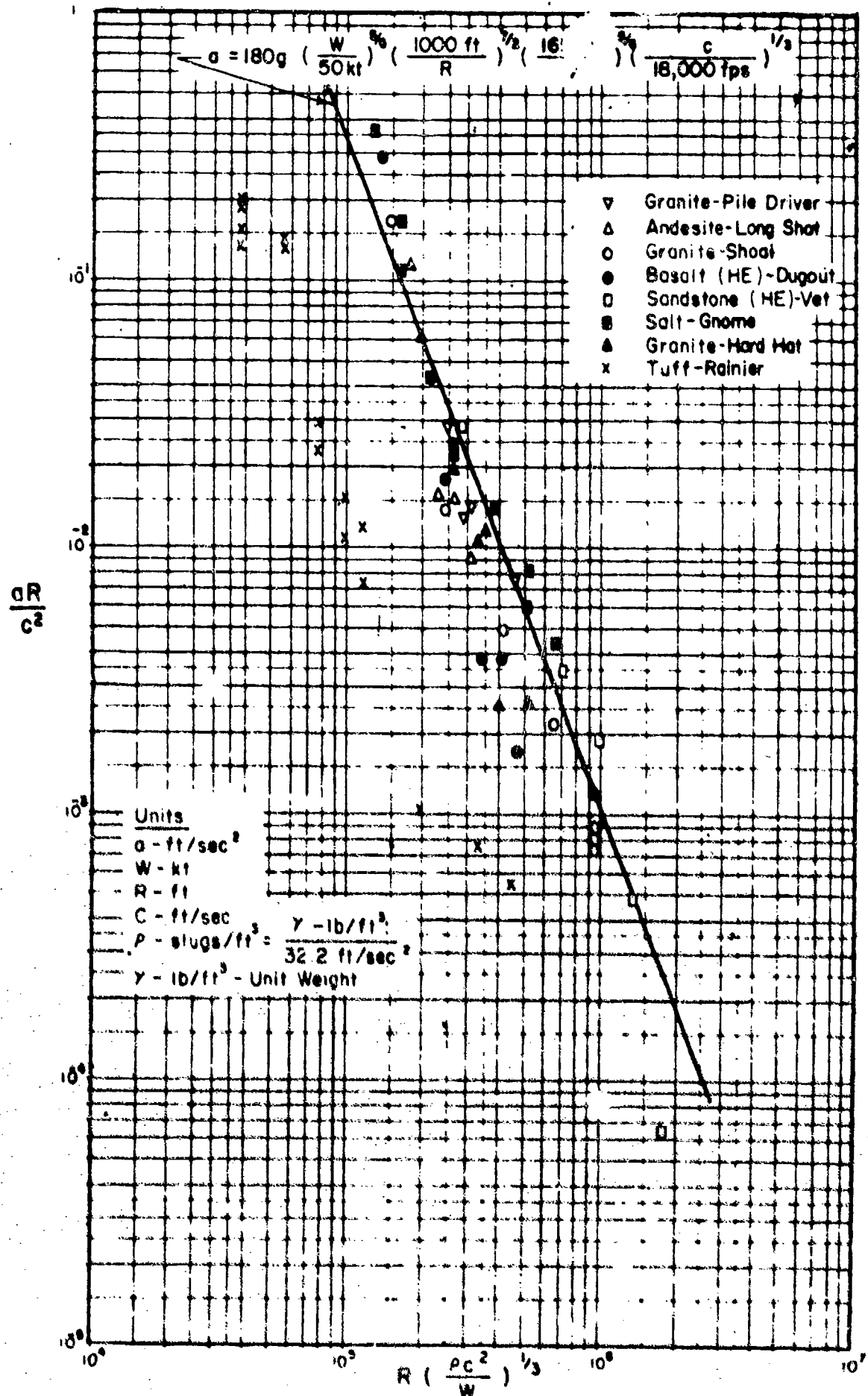


FIG. 4 SCALED ACCELERATION VERSUS SCALED RANGE FOR CONTAINED BURSTS

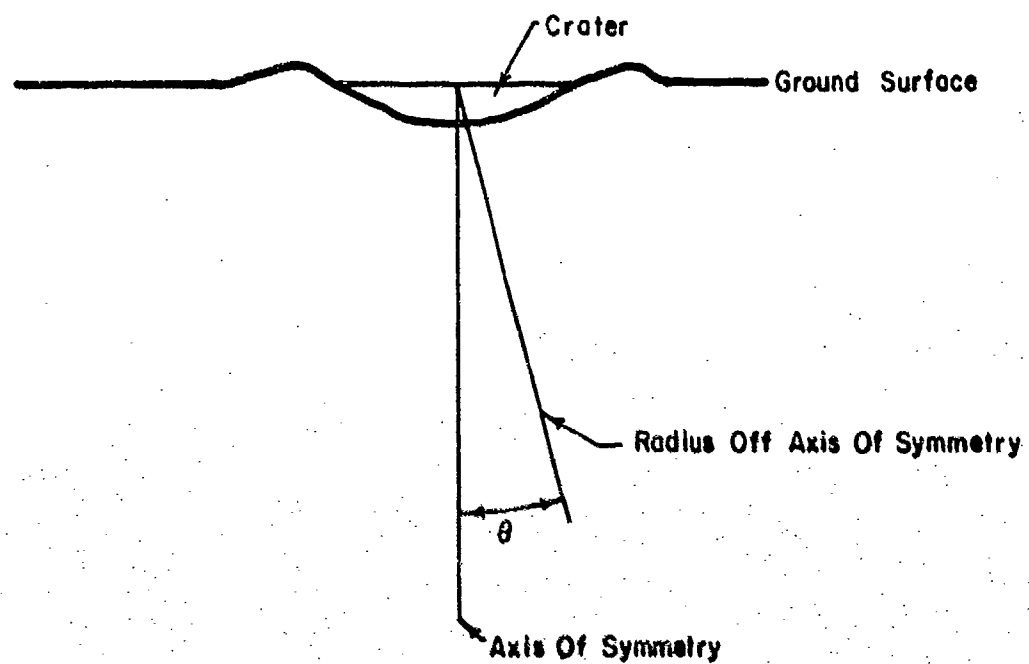


FIG. 5 DEFINITION OF RADIUS ORIENTATION

References

- Murphy, G. (1950), Similitude in Engineering, The Ronald Press Company, New York, New York.
- Newmark, N. M. and Haultiwanger, J. D. (1962), Principles and Practices for Design of Hardened Structures, Technical Documentary Report Number AFSWC-TDR-62-138, Air Force Special Weapons Center, Kirtland Air Force Base, New Mexico.
- Newmark, N. M. (1968), Problems in Wave Propagation in Soil and Rock, In Proc. Intl. Symp. on Wave Propagation and Dynamic Properties of Earth Materials, Univ. of New Mexico Press, Albuquerque, pp. 7-26.
- Cooper, H. F., Brode, H. L., and Leigh (1972), Some Fundamental Aspects of Nuclear Weapons, Technical Report No. AFWL-TR-72-19, Air Force Weapons Laboratory, Air Force Systems Command, Kirtland Air Force Base, New Mexico.
- Trulio, J. G. (1970), Calculations of Cratering, Ejecta, and Dust Lofting, DASA 2507, August 1970.
- Cooper, H. F. (1971), Some Observations on Equivalent Yield, Personal Communication.